

RESEARCH

Open Access



Ultrashort time-to-echo T2* and T2* relaxometry for evaluation of lumbar disc degeneration: a comparative study

Li-Lan Wu¹, Li-Heng Liu^{2,3}, Sheng-Xiang Rao^{2,3}, Pu-Yeh Wu⁴ and Jian-Jun Zhou^{2,3*}

Abstract

Background: To compare potential of ultrashort time-to-echo (UTE) T2* mapping and T2* values from T2*-weighted imaging for assessing lumbar intervertebral disc degeneration (IVDD), with Pfirrmann grading as a reference standard.

Methods: UTE-T2* and T2* values of 366 lumbar discs (L1/2-L5/S1) in 76 subjects were measured in 3 segmented regions: anterior annulus fibrosus, nucleus pulposus (NP), and posterior annulus fibrosus. Lumbar intervertebral discs were divided into 3 categories based on 5-level Pfirrmann grading: normal (Pfirrmann grade I), early disc degeneration (Pfirrmann grades II-III), and advanced disc degeneration (Pfirrmann grades IV-V). Regional differences between UTE-T2* and T2* relaxometry and correlation with degeneration were statistically analyzed.

Results: UTE-T2* and T2* value correlated negatively with Pfirrmann grades ($P < 0.001$). In NP, correlations with Pfirrmann grade were high with UTE-T2* values ($r = -0.733$; $P < 0.001$) and moderate with T2* values ($r = -0.654$; $P < 0.001$). Diagnostic accuracy of detecting early IVDD was better with UTE-T2* mapping than T2* mapping ($P < 0.05$), with receiver operating characteristic analysis area under the curve of 0.715–0.876.

Conclusions: UTE-T2* relaxometry provides another promising magnetic resonance imaging sequence for quantitatively evaluate lumbar IVDD and was more accurate than T2* mapping in the earlier stage degenerative process.

Keywords: Disc degeneration, Lumbar spine, Quantitative magnetic resonance imaging, T2*, UTE-T2*

Introduction

Low back pain (LBP) is a leading cause of disability worldwide, placing a great burden on the global health care system [1, 2]. Intervertebral disc (IVD) degeneration (IVDD) is a significant contributor to nonspecific LBP, with a lifetime prevalence of over 80% [3, 4].

Early stages of IVDD are mainly in the form of biochemical changes, including proteoglycan (PG) reduction, dehydration, and collagen degeneration. It will lead to a decrease in hydrostatic pressure, resulting in nucleus

pulposus (NP) dehydration and loss of the structural and mechanical properties of the IVDs. In advanced stages of IVDD, along with loss of hydration and the subsequent drop in disc pressure, IVD height decreases under load [5–9]. These degenerative changes are accompanied by structural lesions, such as disc herniation, causing LBP, neurogenic claudication, and even cauda equina syndrome. At this stage, treatment strategy is limited to conservative treatment alone or surgical excision [10]. Early detection of alterations in IVDD is important for developing preventative strategies or reestablishing degenerated IVDs, such as gene therapy, stem cell therapy, and growth factor therapy [11–13].

Conventional magnetic resonance imaging (MRI) is widely used for morphologic, qualitative assessment of IVDD in the clinical workup. Lumbar IVDD is

*Correspondence: zhoujianjunzs@126.com

² Department of Radiology, Zhongshan Hospital, Fudan University, Shanghai, China

Full list of author information is available at the end of the article



commonly scored using the Pfirrmann grading system, which is based on the assessment of structure and loss of the signal intensity on T2-weighted imaging (T2WI). This grading system provides a standardized and reliable assessment of MRI disc morphology, but cannot detect early degeneration of IVDs characterized by a loss of PG quantitatively [14, 15].

Several quantitative MRI techniques to evaluate IVD degeneration objectively have been reported, such as diffusion-weighted imaging, diffusion tensor imaging, glycosaminoglycan chemical exchange saturation transfer, sodium, delayed gadolinium-enhanced MRI, T2/T2*, and T1rho mapping. Previous studies have demonstrated that T2* mapping could be quantitative imaging biomarkers for evaluating the biochemical state of the discs and correlating that with histology, water content, and degeneration [16].

Ultrashort time-to-echo (UTE) imaging as a novel MRI technique has the capacity to catch very short T2* signals (0.008~0.50 ms) [17–20]. It has been confirmed to be sensitive to changes in the deep tissue matrix and to subtle and even preclinical degeneration [21]. To date, UTE-T2* imaging has been reported to be a reliable tool for quantitative assessment of the biochemical changes of short T2 tissues, including tendon, cartilage, and ligament, etc. [20–25]. However, to the best of our knowledge, studies on UTE-T2* quantitative technique in evaluating IVDD are scarce. We hypothesized that quantitative UTE-T2* mapping is capable of revealing degenerative changes in the discs.

The present study aimed to assess whether lumbar IVDD can be evaluated using UTE-T2* mapping and to compare the potential of UTE-T2* and T2* values in the diagnosis of early IVDD.

Materials and methods

Subjects

Ethics approval for this study was provided by the ethics commission of the Fudan University Affiliated Zhongshan Hospital Xiamen Branch. Written informed consent

was obtained from all subjects. The inclusion criteria were patients with single or recurrent episodes of non-specific LBP in the last 6 months and age ≥ 18 years. Exclusion criteria were contraindications for MRI and patients with other spine diseases, such as spinal infection, tumor, tuberculosis, and serious scoliosis.

MRI protocols

All data were acquired on a 3.0 T MRI scanner (Discovery™ MR750w, GE Healthcare, Milwaukee, WI) equipped with an 8-channel spine-array coil covering the IVDs L1/L2 to L5/S1. All participants underwent MRI examinations, including sagittal T2WI, UTE-T2*, and T2* mapping. T2WI images were used for Pfirrmann grading. Detailed acquisition parameters were assigned to T2WI, UTE-T2* mapping, and T2* mapping.

For T2WI, repetition time (TR)/echo time (TE)=2500/120 ms, slice thickness/gap=5/0.5 mm, field of view (FOV)=300×300 mm, matrix=256×192, and bandwidth=41.7 kHz. For UTE-T2* mapping, TR=112.4 ms, TE=0.032/3.8/8.8/13.2 ms, slice thickness/gap=3/0.5 mm, flip angle=15, FOV=300×300 mm, matrix=300×256, and bandwidth=62.5 kHz. Maps of the T2* was calculated using $R2^*(R2^*=1/T2^*)$ [26, 27]. For R2* mapping, TR=12.5 ms, TE=1.40 /2.29 /3.18/4.07/ 4.96/5.85/ 6.74 / 7.63 / 8.52 ms, slice thickness/gap=5/0 mm, flip angle=5, FOV=300×300 mm, matrix=256×192, and bandwidth=111.1 kHz.

Image analysis

All lumbar IVDs were evaluated by 2 musculoskeletal radiologists each with more than six years of experience using T2WI and assigned a Pfirrmann grade (Table 1) [28]. Disc degenerations also were divided into three categories [11]: normal (Pfirrmann grade I), early disc degeneration (Pfirrmann grade II–III), and advanced disc degeneration (Pfirrmann grade IV–V). UTE-T2* values were calculated by mono-exponential fitting using custom code in MATLAB (MathWorks,

Table 1 Pfirrmann grades of disc degeneration

Grade	Structure	Distinction of nucleus and annulus	Signal intensity	Height of intervertebral disc
I	Homogeneous, bright white	Clear	Hyperintense, isointense to cerebrospinal fluid	Normal
II	Inhomogeneous with or without horizontal bands	Clear	Hyperintense, isointense to cerebrospinal fluid	Normal
III	Inhomogeneous, gray	Unclear	Intermediate	Normal to slightly decreased
IV	Inhomogeneous, gray to black	Lost	Intermediate to hypointense	Normal to moderately decreased
V	Inhomogeneous, black	Lost	Hypointense	Collapsed disc space

Natick, MA). Five circular regions of interest (ROIs) of equal size were manually drawn on the midline slice of sagittal UTE-T2* and T2* mappings from anterior to posterior (**Fig. 1**), including the anterior annulus fibrosus (AAF; ROI 1), nucleus pulposus (NP; ROI 2–4), and posterior annulus fibrosus (PAF; ROI 5) [29].

Statistical analysis

Statistical analysis was conducted using SPSS 22.0 software (IBM, Armonk, NY) and Medcalc 20.022 (Mariakerke, Belgium). The Kruskal–Wallis test was performed to determine differences among the 5-level Pfirrmann grades. The differences between the two methods were expressed using the $\pm 95\%$ confidence intervals (CIs) from the Bland–Altman analysis. Correlations of quantitative values with Pfirrmann grades were analyzed using Spearman's rank correlation. Receiver operating characteristic (ROC) analysis was performed and area under the curve (AUC), sensitivity, specificities, positive likelihood ratio (+LR), and negative likelihood ratio (–LR) were obtained to assess the diagnostic efficacy of each quantitative parameter for differentiating normal IVDs from early disc degeneration and to differentiate early disc degeneration from advanced disc degeneration. AUCs were compared using the DeLong method [30]. A *P* value less than 0.05 was considered statistically significant.

Results

Clinical characteristics

Seventy-six subjects aged 54.4 ± 15.7 years (range, 19–85 years) were recruited into this study. They included 29 males (aged 51.8 ± 17.2 years; range, 19–82 years) and 47 females (aged 54.5 ± 14.9 years; range, 27–85 years). Five intervertebral discs (L1/L2–L5/S1) per subject were examined, of which 14 discs were excluded due to previous vertebral fusion operation ($n=2$), collapsed disc space (Pfirrmann grade V) that made it impossible to measure the quantitative values ($n=9$), and image quality problems ($n=3$). A total of 366 IVDs were included in this study.

Using the Pfirrmann grading system, 73 discs were categorized as grade I; 110 discs, as grade II; 164 discs, as grade III; and 19 discs, as grade IV. The flowchart for the enrollment of the study population is presented in **Fig. 2**. The distribution of the UTE-T2* and T2* values with respect to Pfirrmann grades is provided in **Table 2**.

Correlation of UTE-T2* and T2* values with Pfirrmann grades

The Kruskal–Wallis test demonstrated that all quantitative values for all segments were significantly different among different Pfirrmann grades (**Table 2**). Bland–Altman plots are shown in **Fig. 3**. There was no significant bias between UTE-T2* and T2* values in NP and PAF ($P > 0.05$). UTE-T2* values showed high

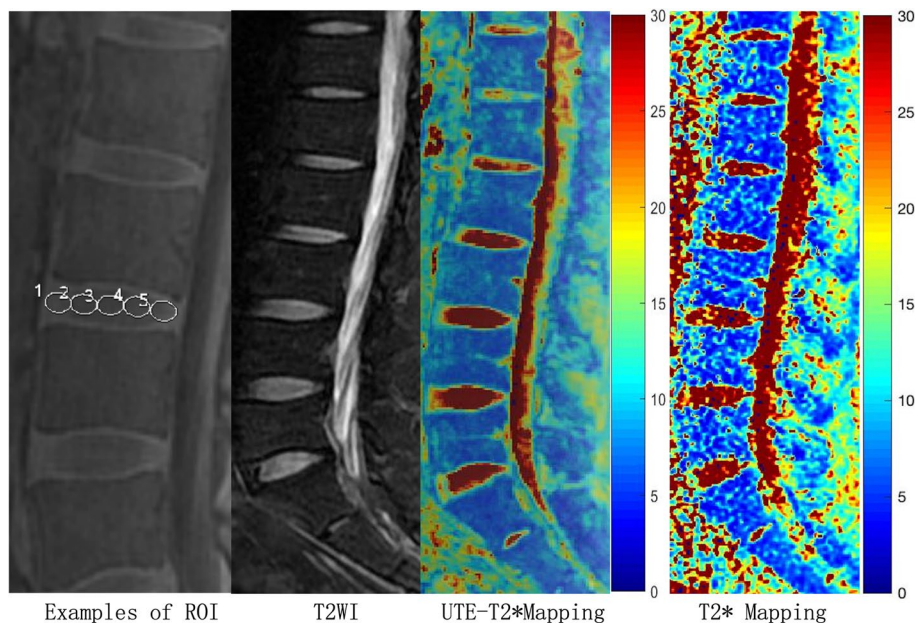


Fig. 1 MR images of the lumbar spine of a 39-year-old woman. Every lumbar IVD was cut into 5 uniform parts in each UTE-T2* and T2* mapping. An ROI of 1 represented AAF, ROI 2–4 represented NP, and ROI 5 represented PAF. IVD, intervertebral disc; NP, nucleus pulposus; PAF, posterior annulus fibrosus; ROI, region of interest; UTE, ultrashort time-to-echo

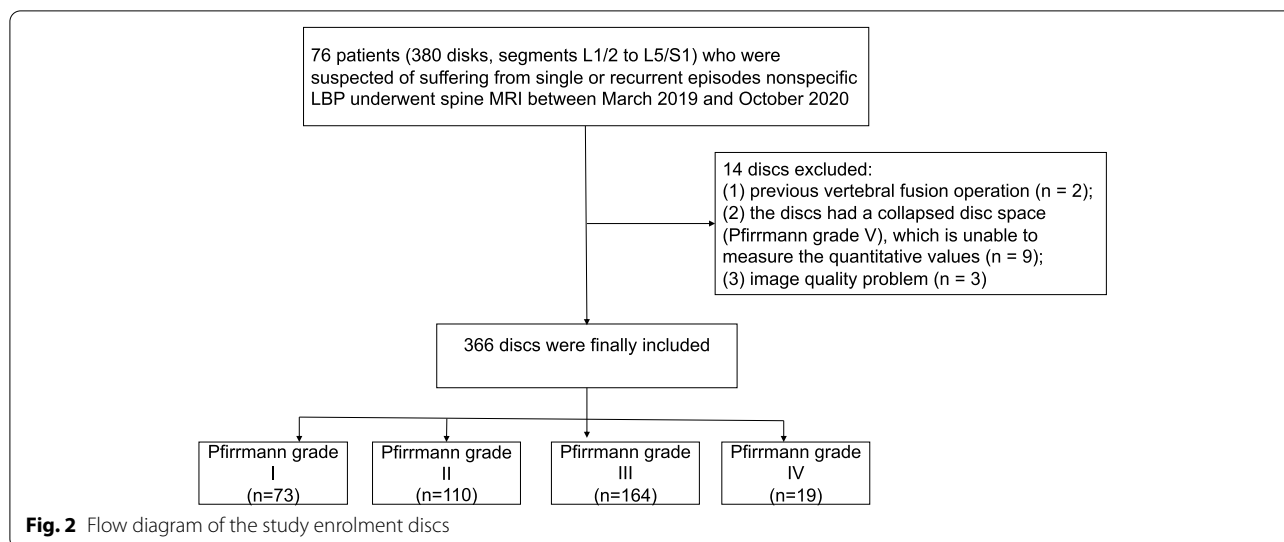


Table 2 UTE-T2* and T2* values of AAF, NP, and PAF in each Pfirrmann grades

Number		Pfirrmann grade				P value
		I 73	II 110	III 164	IV 19	
AAF	UTE-T2*	23.5 ± 5.6	19.9 ± 4.7	19.2 (5.8)	15.9 ± 3.4	< 0.001
	T2*	21.2 (8.0)	20.0 (7.4)	16.9 (5.9)	16.2 (11.1)	< 0.001
NP	UTE-T2*	46.6 ± 10.1	35.9 (9.9)	27.8 ± 5.9	20.0 ± 5.3	< 0.001
	T2*	48.3 (19.9)	43.3 (17.8)	29.7 (9.9)	22.8 ± 5.8	< 0.001
PAF	UTE-T2*	24.6 ± 3.6	20.6 ± 5.7	18.7 (6.5)	11.9 (8.3)	< 0.001
	T2*	19.7 ± 4.8	17.3 (7.0)	15.2 (5.4)	11.8 (6.3)	< 0.001

AAF Anterior annulus fibrosus, NP Nucleus pulposus, PAF Posterior annulus fibrosus, UTE Ultrashort time-to-echo distribution data is expressed as mean ± standard deviation skewed data is expressed as median, quartile spacing UTE-T2* and T2* value is given in ms

correlations with Pfirrmann grade in NP ($r = -0.733$; $P < 0.001$). Moderate correlations with Pfirrmann grade were observed in T2* value of NP ($r = -0.654$; $P < 0.001$). Comparing the Spearman correlation coefficient, the highest correlation value was seen in NP and the lowest was seen in AAF. Among those, the UTE-T2* value of NP showed the highest correlation values with Pfirrmann grades. Results of Spearman’s correlation analysis are summarized in **Fig. 4**.

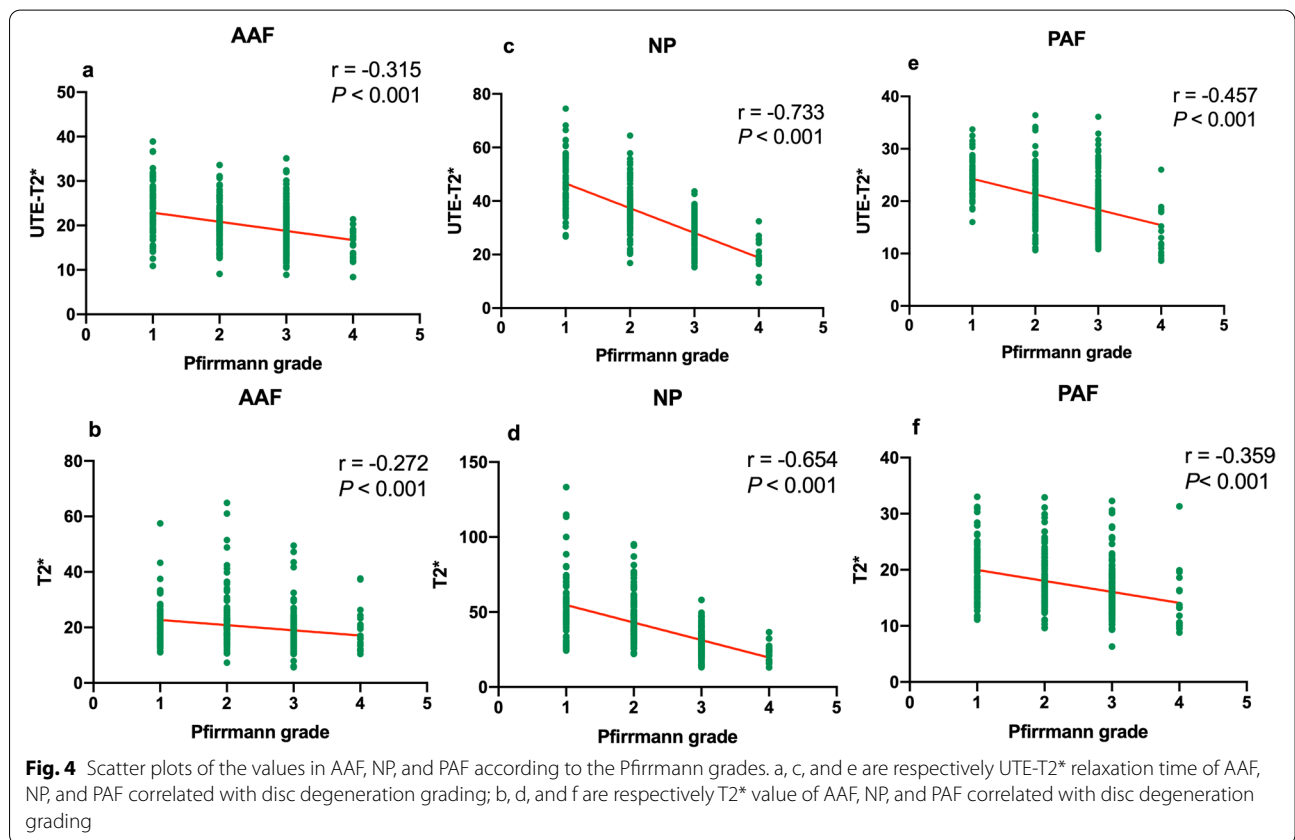
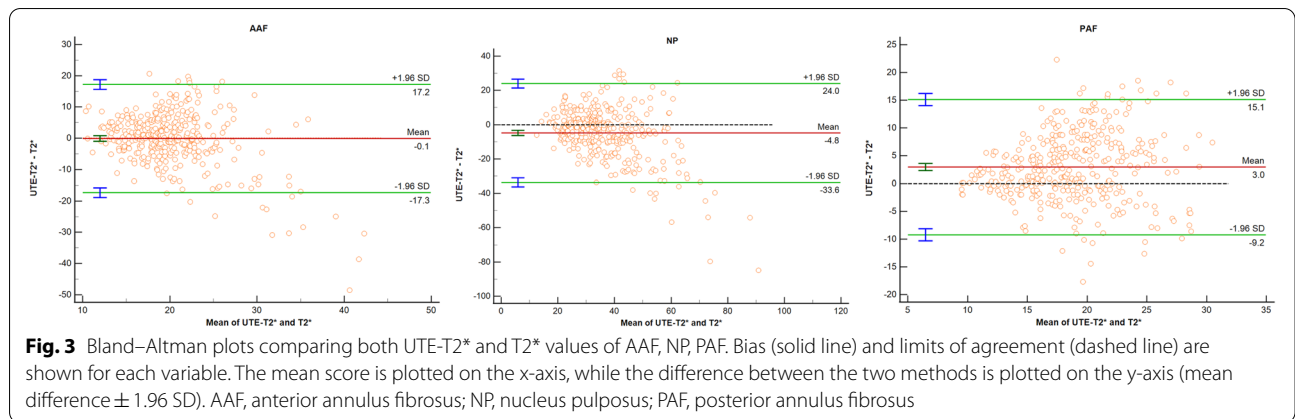
Post hoc multiple comparisons among each Pfirrmann grades

There were significant differences in UTE-T2* values of NP and PAF between each Pfirrmann grade. T2* values were found to be significantly different between

Pfirrmann grade II and grade III in AAF, NP, and PAF (**Fig. 5**).

Diagnostic performance of UTE-T2* and T2* values in distinguishing each degeneration groups

ROC curves of UTE-T2* and T2* values for distinguishing each degeneration groups are plotted in **Fig. 6** The corresponding diagnostic test characteristics are provided in **Table 3**. The AUC values of UTE-T2* mapping in AAF, NP, and PAF were 0.715, 0.876, 0.787, respectively, for identification of the early disc degeneration, and 0.726, 0.893, 0.804, respectively, for identification of the advanced disc degeneration. The AUC values of T2* mapping in AAF, NP, and PAF were 0.620, 0.763, 0.670, respectively, for identification of the early disc

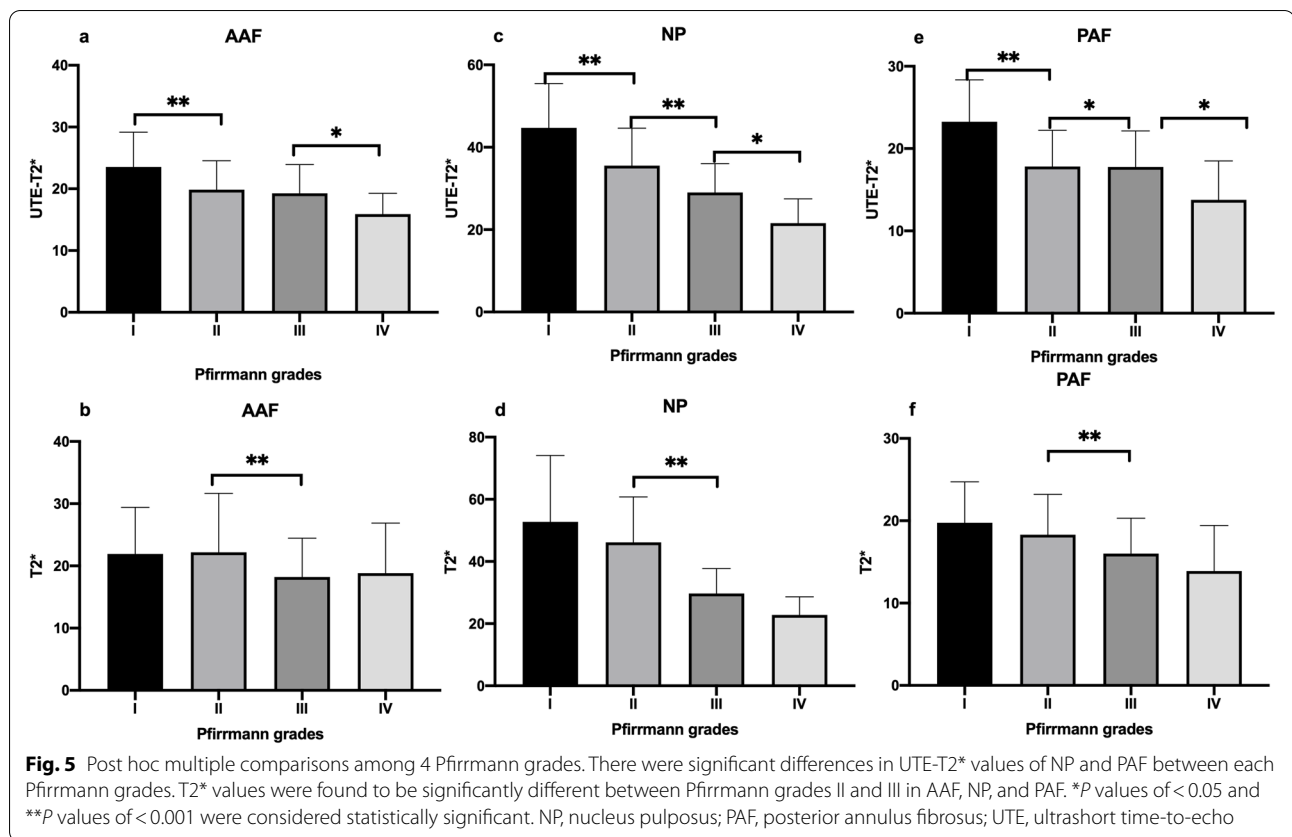


degeneration, and 0.570, 0.842, 0.720, respectively, for identification of the advanced disc degeneration.

For pairwise comparisons of ROC curves, UTE-T2* values in NP and PAF were better in identifying early degeneration IVDs than those in T2*. There were no significant differences among UTE-T2* and T2* mapping in AAF. Comparing between different segments, diagnostic performance of NP was the highest in predicting the early degeneration IVDs, AAF and PAF performed similarly.

For differentiating early and advanced disc degeneration, the UTE-T2* value of PAF was better than that of T2* and there were no significant differences among UTE-T2* and T2* mapping in AAF and NP. Comparing between different segments, diagnostic performance of NP was better than AAF, AAF and PAF performed similarly in predicting the advanced disc degeneration.

Overall, the diagnostic efficacy of UTE T2* mapping was better than that of T2* mapping for evaluating



IVDD, especially in NP. The results of this study demonstrated that the UTE-T2* value in NP showed high correlations with Pfirrmann grade ($r = -0.733$; $P < 0.001$) and that AUCs for the assessment of the early disc degeneration (AUC 0.876) were significantly higher than those for T2* (AUC 0.763).

Discussion

This study is the first to investigate and compare the diagnostic efficacies of UTE-T2* and T2* mapping in detecting IVDD in humans. The results may help to confirm the feasibility and specificity of UTE-T2* as an objective and quantitative tool to identify early degenerative changes of the disc and show promise for clinicians to modify the diagnostics and therapeutic management strategies more accurately.

Conventional MRI, such as the Pfirrmann scale with T2WI, was limited in detecting ultrastructural alterations of early IVDD. Early stages of disc degeneration include biochemical changes, such as a loss or reduction of PG content, which can ultimately lead to dehydration. T2 relaxation reflected the integrated environment of the IVD, including water, protein, collagen, and other solutes [31], and was sensitive to water content and the composition of the collagen network

structure. Researchers have reported that T2* relaxation time showed a good correlation with PG and collagen contents in 18 humans cadaveric IVDs [32]. Our findings confirmed an increase in the quantitative T2* values between the AAF and NP and a decrease between the NP and the PAF. In line with an earlier report [33, 34], T2 and T2* mapping provided roughly similar results. The inverse correlation of the T2 relaxation time in the disc with Pfirrmann grade has been reported by Welsch et al. [35] and Noebauer et al. [36], the early study reported a low-to-moderate correlation between Pfirrmann grades and T2 relaxation times, which were consistent with the Spearman's correlation coefficient between Pfirrmann grades and T2* value in our results. Both T2 and T2* mapping differ in the biochemical sensitivity of disc tissue, with T2 mapping being sensitive to tissue hydration, while T2* mapping being more sensitive to changes in tissue integrity [35]. T2* mapping provide more valuable biochemical information on the IVDs ultrastructure, together with three-dimensional acquisition capability and higher spatial resolution in a short scan time [37].

UTE-T2* mapping was acquired using different echo times in the short (1–10 ms) and ultrashort echo time range [19, 22]. Because UTE-T2* mapping can catch the

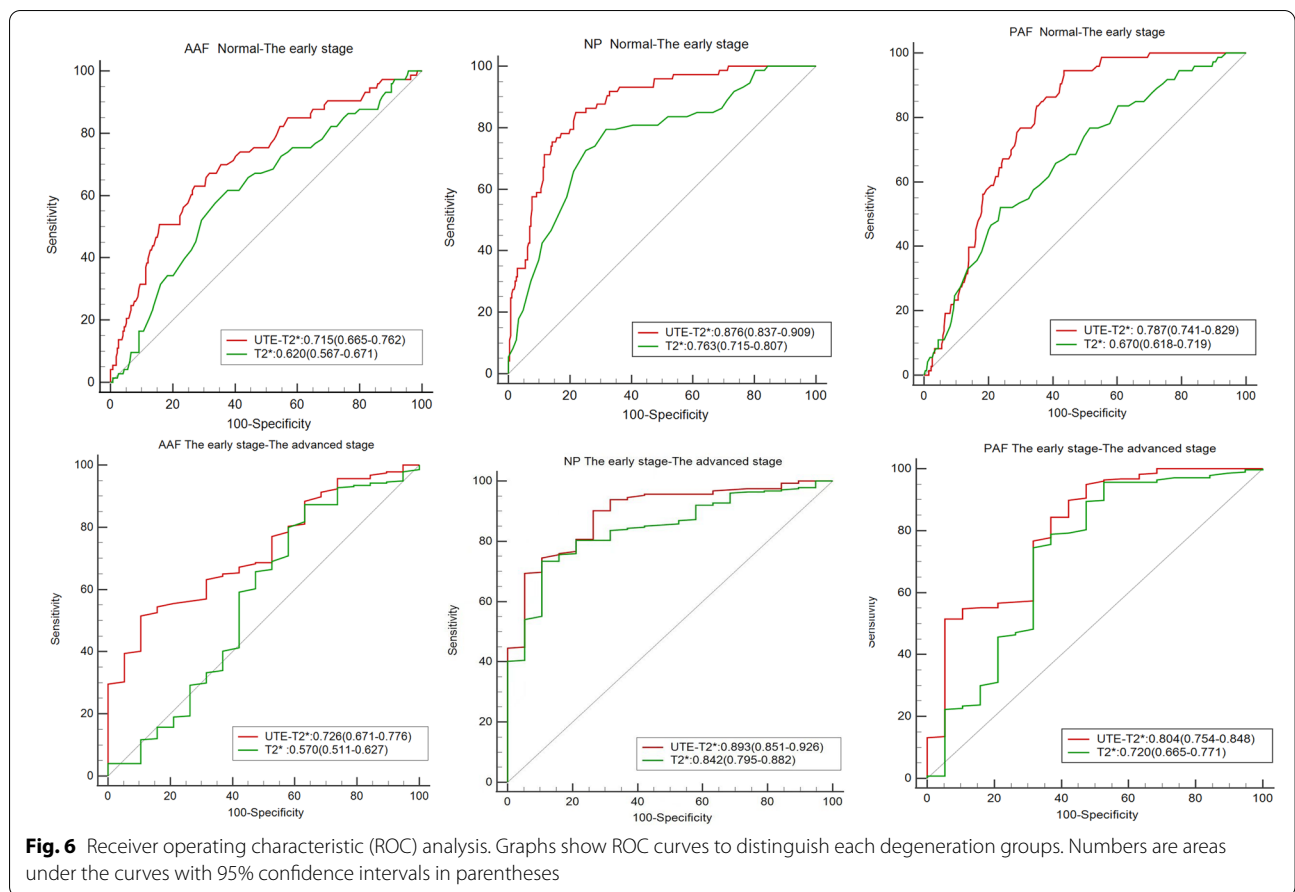


Table 3 Diagnostic performance of UTE-T2* and T2* values in distinguishing degeneration groups

3a. Normal-The early stage		AUC (95% CI)	Sensitivity (%)	Specificity (%)	+LR	-LR	Cutoff
AAF	UTE-T2*	0.715 (0.665–0.762)	73.0	63.0	1.97	0.43	≤ 21.8
	T2*	0.620 (0.567–0.671)	66.1	58.9	1.61	0.58	≤ 20.1
NP	UTE-T2*	0.876 (0.837–0.909)	78.1	84.9	5.18	0.26	≤ 36.7
	T2*	0.763 (0.715–0.807)	68.3	79.5	3.32	0.40	≤ 39.2
PAF	UTE-T2*	0.787 (0.741–0.829)	56.6	94.5	10.32	0.46	≤ 19.6
	T2*	0.670 (0.618–0.719)	76.3	52.1	1.59	0.46	≤ 19.4
3b. The early stage – The advanced stage		AUC (95% CI)	Sensitivity (%)	Specificity (%)	+LR	-LR	Cutoff
AAF	UTE-T2*	0.726 (0.671–0.776)	89.5	51.5	1.84	0.20	≤ 19.1
	T2*	0.570 (0.511–0.627)#	36.8	87.2	2.88	0.72	≤ 13.6
NP	UTE-T2*	0.893 (0.851–0.926)	94.7	69.3	3.09	0.08	≤ 27.0
	T2*	0.842 (0.795–0.882)	89.5	73.4	3.36	0.14	≤ 27.4
PAF	UTE-T2*	0.804 (0.754–0.848)	57.9	89.8	5.67	0.47	≤ 13.0
	T2*	0.720 (0.665–0.771)	47.4	95.6	10.82	0.55	≤ 10.6

P values of > 0.05 were considered without statistical significance

UTE-T2* and T2* value is given in ms

short T2* relaxations from tissues, it is more sensitive to biochemical collagen matrix changes compared with conventional MRI techniques, based on histologic standards [19].

Multiple large general-population-based studies have proved that UTE-T2* mapping can detect cartilage subsurface matrix changes, which can be indicative of reduced cartilage health from injury or early degeneration noninvasively [20, 23, 25]. Similar to the results reported by Detiger et al. [16], we observed a trend of decreasing UTE-T2* value with increasing degree of degeneration. The previous study revealed a significant correlation between T2* relaxation time and glycosaminoglycans (GAG) content in the nucleus pulposus, as well as histologic scoring with varying grades of degeneration [16]. During the aging process, the quantity and quality of PG and collagen contents diminish, along with a decrease in short T2* signal accordingly [21, 25, 34, 38]. T2* relaxometry appeared to be sensitive to water and PG contents. This may be the initial step in the degenerative cycle [25, 34, 38], which could be the underlying reasons for the decreased UTE-T2* and T2* value.

In NP and PAF, UTE-T2* mapping showed significantly higher diagnostic accuracy in differentiating early disc degeneration from normal than did T2*. Theoretically, both UTE-T2* and T2* mapping measured the T2* value of the tissue. UTE MRI technique mitigates the rapid signal loss from short T2* by reducing the TE to the scale of 0–200 microseconds to sample the free induction decay as early as possible. With considerably shorter TEs (0.032 ms in this study) than T2*, UTE-T2* mapping allows signals from very short T2 components to be detected [23]. Thus, UTE-T2* mapping is less sensitive to the magic angle effect and more sensitive to water protons and their local environment, making it a satisfactory method for evaluating disc degeneration. Because T2* relaxation time has been reported to reflect both the water content and PG content reduction [16], it is not hard to understand why the UTE-T2* value has better diagnostic accuracy than T2* for differentiating early disc degeneration.

Previous studies have reported that T2 relaxation time of Pfirrmann grades IV is significantly shorter than Pfirrmann grades III, and no significant differences were found between Pfirrmann grades IV and V, both of which show extremely low signal intensity [39]. The results of our study showed that compared to T2* values, UTE-T2* values conveyed significantly higher diagnostic performance in distinguishing the early disc degeneration from the advanced in PAF. Takashima et al. [40] reported that short T2* relaxation times with UTE are promising for assessing progressive IVD degeneration with poor water content, such as fibrosis change of IVDD with short T2

relaxation time. Our results are consistent with those findings quantitatively. Takashima et al. did not further discuss the quantitative evaluation of the early disc degeneration because their study population did not include grade I IVDs. Our results would appear to complement and refine their research.

A previous report on healthy ovine IVDs demonstrated that the T2 values show regional variation in discs and reported that high T2 values were observed in NP and low T2 values in the AAF and PAF when histologically evaluated [41]. Disc degeneration is believed to originate in NP with depletion of GAG, followed by a reduction in water content [5, 42]. Similar to previous reports, our study showed that correlations with Pfirrmann grade and UTE-T2* and T2* values were highest in NP and lowest in AAF. Our results also showed that NP had the highest diagnostic accuracy in predicting the early degeneration IVDs, while AFP and PFP were similar in predicting the early degeneration IVDs. These results suggest that the destruction of hydrophilic GAGs within NP was the main cause of the accumulation of cleaved extracellular matrix fragments with disc aging [16].

There were some limitations in this study. First, our study had no detailed histologic confirmation associated with IVDD changes. This is hard to achieve in humans. In addition, the relationship between T2* values and biochemical changes in IVDD has been previously established in human cadaveric lumbar discs [32]. Second, we were unable to compare the related clinical symptoms with the degree of degeneration in MRI quantitative parameters. Future research is warranted to explore these ideas. Third, no patient in this study showed grade V IVDs because grade V IVDs tend to have a collapsed disc space or a vacuum phenomenon, which is unable to measure the quantitative values due to susceptibility artifacts. If the complete grade V IVDs data set were available, quantitative evaluation of advanced IVD degeneration could be closer to reality. However, as our principal purpose was to detect early disc degeneration, the impact of incomplete grade V IVDs dataset on our results is within acceptable limits.

Conclusions

We demonstrated that UTE-T2* mapping was more accurate than T2* mapping in quantitatively diagnosing early intervertebral disc degeneration. In particular, UTE-T2* mapping allowed for precisely distinguishing disc degeneration, potentially providing a promising imaging biomarker with potential applications in intervertebral disc degeneration for the emerging cell-based therapies.

Abbreviations

LBP: Low back pain; IVD: Intervertebral disc; IVDD: Intervertebral disc degeneration; PG: Proteoglycan; NP: Nucleus pulposus; T2WI: T2-weighted imaging; UTE: Ultrashort time-to-echo; TR: Repetition time; TE: Echo time; FOV: Field of view; PAF: Posterior annulus fibrosus; AAF: Anterior annulus fibrosus; ROI: Region of interest; ROC: Receiver operating characteristic.

Acknowledgements

The authors would like to thank patients from Fudan University Affiliated Zhongshan Hospital Xiamen Branch for their participation in the study.

Authors' contributions

Li-Heng Liu contributed to study design, Jian-Jun Zhou conceived and designed the study; Li-Lan Wu performed the study, analyzed the data and wrote the paper. Sheng-Xiang Rao and Pu-Yeh Wu contributed to critical revisions of the manuscript. All authors approved the final version of the manuscript.

Funding

The study received statutory funding from the Science and Technology Guided Project of Fujian Province, China(Grant No. 2019D025);no additional funding was received.

Availability of data and materials

The datasets generated and/or analysed during the current study are available from the corresponding author on reasonable request.

Declarations

Ethics approval and consent to participate

The subjects were informed of the study goals and test protocols before giving their signed informed consent for participation. The study protocol received approval from the Local Bioethics Committee (certificate of approval No. B2021-007) of the Fudan University Affiliated Zhongshan Hospital Xiamen Branch in Fujian (China) according to the principles and policies of the Declaration of Helsinki. All methods were performed in accordance with the relevant guidelines and regulations in the Ethics approval and consent to participate.

Consent for publication

Informed consent to publish was obtained from the participants for publication of the images.

Competing interests

The authors declare no conflict of interest.

Author details

¹Department of Radiology, Xiamen Branch, Zhongshan Hospital, Fudan University, Xiamen, China. ²Department of Radiology, Zhongshan Hospital, Fudan University, Shanghai, China. ³Shanghai Institute of Medical Imaging, Shanghai, China. ⁴GE Healthcare, Beijing, China.

Received: 19 March 2022 Accepted: 24 May 2022

Published online: 01 June 2022

References

- Bardin LD, King P, Maher CG. Diagnostic triage for low back pain: a practical approach for primary care. *Med J Aust.* 2017;206:268–73. <https://doi.org/10.5694/mja16.00828>.
- Ogon I, et al. Imaging diagnosis for intervertebral disc. *JOR Spine.* 2020;3:e1066. <https://doi.org/10.1002/jsp2.1066>.
- Liao Z, et al. Exosomes from mesenchymal stem cells modulate endoplasmic reticulum stress to protect against nucleus pulposus cell death and ameliorate intervertebral disc degeneration in vivo. *Theranostics.* 2019;9:4084–100. <https://doi.org/10.7150/thno.33638>.
- Bashkuev M, Reitmaier S, Schmidt H. Relationship between intervertebral disc and facet joint degeneration: a probabilistic finite element model study. *J Biomech.* 2020;102:109518. <https://doi.org/10.1016/j.jbiomech.2019.109518>.
- Zeng F, et al. A comparative study of diffusion kurtosis imaging and T2* mapping in quantitative detection of lumbar intervertebral disk degeneration. *Eur Spine J.* 2019;28:2169–78. <https://doi.org/10.1007/s00586-019-06007-z>.
- Griffith JF, et al. Modified Pfirrmann grading system for lumbar intervertebral disc degeneration. *Spine (Phila Pa 1976).* 2007;32:E708–712. <https://doi.org/10.1097/BRS.0b013e31815a59a0>.
- Menezes-Reis R, et al. Lumbar intervertebral discs T2 relaxometry and T1 ρ relaxometry correlation with age in asymptomatic young adults. *Quant Imaging Med Surg.* 2016;6:402–12. <https://doi.org/10.21037/qims.2016.08.01>.
- Wang F, et al. A histocytological and radiological overview of the natural history of intervertebral disk: from embryonic formation to age-related degeneration. *Eur Spine J.* 2019;28:633–48. <https://doi.org/10.1007/s00586-019-05903-8>.
- Yang B, Wendland MF, O'Connell GD. Direct quantification of intervertebral disc water content using MRI. *J Magn Reson Imaging.* 2020;52:1152–62. <https://doi.org/10.1002/jmri.27171>.
- Gugliotta M, et al. Surgical versus conservative treatment for lumbar disc herniation: a prospective cohort study. *BMJ Open.* 2016;6:e012938. <https://doi.org/10.1136/bmjopen-2016-012938>.
- Wu, PH., Kim, HS. & Jang, IT. 2020 Intervertebral Disc Diseases PART 2: A Review of the Current Diagnostic and Treatment Strategies for Intervertebral Disc Disease. *Int J Mol Sci* 21. <https://doi.org/10.3390/ijms21062135>.
- Tong W, et al. Cell therapy for the degenerating intervertebral disc. *Transl Res.* 2017;181:49–58. <https://doi.org/10.1016/j.trsl.2016.11.008>.
- Roh, EJ. et al. 2021. Genetic Therapy for Intervertebral Disc Degeneration. *Int J Mol Sci* 22. <https://doi.org/10.3390/ijms22041579>
- Zobel BB, et al. T1 ρ magnetic resonance imaging quantification of early lumbar intervertebral disc degeneration in healthy young adults. *Spine (Phila Pa 1976).* 2012;37:1224–30. <https://doi.org/10.1097/BRS.0b013e31824b2450>.
- Togao O, et al. A qualitative and quantitative correlation study of lumbar intervertebral disc degeneration using glycosaminoglycan chemical exchange saturation transfer, pfirrmann grade, and T1- ρ AJNR. *Am J Neuroradiol.* 2018;39:1369–75. <https://doi.org/10.3174/ajnr.A5657>.
- Detiger SE, et al. MRI T2* mapping correlates with biochemistry and histology in intervertebral disc degeneration in a large animal model. *Eur Spine J.* 2015;24:1935–43. <https://doi.org/10.1007/s00586-014-3498-1>.
- Chang EY, Du J, Bae WC, Chung CB. Qualitative and quantitative ultrashort echo time imaging of musculoskeletal tissues. *Semin Musculoskelet Radiol.* 2015;19:375–86. <https://doi.org/10.1055/s-0035-1563733>.
- Du J, Takahashi AM, Chung CB. Ultrashort TE spectroscopic imaging (UTESI): application to the imaging of short T2 relaxation tissues in the musculoskeletal system. *J Magn Reson Imaging.* 2009;29:412–21. <https://doi.org/10.1002/jmri.21465>.
- Chang EY, Du J, Chung CB. UTE imaging in the musculoskeletal system. *J Magn Reson Imaging.* 2015;41:870–83. <https://doi.org/10.1002/jmri.24713>.
- Qiao Y, et al. UTE-T2* analysis of diseased and Healthy achilles tendons and correlation with clinical score: an in vivo preliminary study. *Biomed Res Int.* 2017;2017:2729807. <https://doi.org/10.1155/2017/2729807>.
- Chu CR, et al. Quantitative magnetic resonance imaging UTE-T2* mapping of cartilage and meniscus healing after anatomic anterior cruciate ligament reconstruction. *Am J Sports Med.* 2014;42:1847–56. <https://doi.org/10.1177/0363546514532227>.
- Xie Y, et al. Quantitative magnetic resonance imaging UTE-T2* mapping of tendon healing after arthroscopic rotator Cuff repair: a longitudinal study. *Am J Sports Med.* 2020;48:2677–85. <https://doi.org/10.1177/0363546520946772>.
- Yang J, et al. Quantitative ultrashort echo time magnetization transfer (UTE-MT) for diagnosis of early cartilage degeneration: comparison with UTE-T2* and T2 mapping. *Quant Imaging Med Surg.* 2020;10:171–83. <https://doi.org/10.21037/qims.2019.12.04>.
- Williams AA, Titchenal MR, Do BH, Guha A, Chu CR. MRI UTE-T2* shows high incidence of cartilage subsurface matrix changes 2 years after ACL reconstruction. *J Orthop Res.* 2019;37:370–7. <https://doi.org/10.1002/jor.24110>.

25. Titchenal MR, et al. Cartilage subsurface changes to magnetic resonance imaging UTE-T2* 2 years after anterior cruciate ligament reconstruction correlate with walking Mechanics associated with knee osteoarthritis. *Am J Sports Med.* 2018;46:565–72. <https://doi.org/10.1177/0363546517743969>.
26. Ogawa S, et al. Functional brain mapping by blood oxygenation level-dependent contrast magnetic resonance imaging. A comparison of signal characteristics with a biophysical model. *Biophys J.* 1993;64:803–12. [https://doi.org/10.1016/s0006-3495\(93\)81441-3](https://doi.org/10.1016/s0006-3495(93)81441-3).
27. Kühn JP, et al. Proton-density fat fraction and simultaneous R2* estimation as an MRI tool for assessment of osteoporosis. *Eur Radiol.* 2013;23:3432–9. <https://doi.org/10.1007/s00330-013-2950-7>.
28. Pfirrmann CW, Metzendorf A, Zanetti M, Hodler J, Boos N. Magnetic resonance classification of lumbar intervertebral disc degeneration. *Spine (Phila Pa 1976).* 2001;26:1873–8. <https://doi.org/10.1097/00007632-200109010-00011>.
29. Mok GSP, et al. Comparison of three approaches for defining nucleus pulposus and annulus fibrosus on sagittal magnetic resonance images of the lumbar spine. *J Orthop Translat.* 2016;6:34–41. <https://doi.org/10.1016/j.jot.2016.02.003>.
30. DeLong ER, DeLong DM, Clarke-Pearson DL. Comparing the areas under two or more correlated receiver operating characteristic curves: a non-parametric approach. *Biometrics.* 1988;44:837–45.
31. Chai JW, Kang HS, Lee JW, Kim SJ, Hong SH. Quantitative analysis of disc degeneration using axial T2 mapping in a percutaneous annular puncture model in rabbits. *Korean J Radiol.* 2016;17:103–10. <https://doi.org/10.3348/kjr.2016.17.1.103>.
32. Ellingson AM, Nagel TM, Polly DW, Ellermann J, Nuckley DJ. Quantitative T2* (T2 star) relaxation times predict site specific proteoglycan content and residual mechanics of the intervertebral disc throughout degeneration. *J Orthop Res.* 2014;32:1083–9. <https://doi.org/10.1002/jor.22633>.
33. Cui YZ, Yang XH, Liu PF, Wang B, Chen WJ. Preliminary study on diagnosis of lumbar disc degeneration with magnetic resonance T1p, T2 mapping and DWI quantitative detection technologies. *Eur Rev Med Pharmacol Sci.* 2016;20:3344–50.
34. Imanishi T, Akeda K, Murata K, Sudo A. Effect of diminished flow in rabbit lumbar arteries on intervertebral disc matrix changes using MRI T2-mapping and histology. *BMC Musculoskelet Disord.* 2019;20:347. <https://doi.org/10.1186/s12891-019-2721-y>.
35. Welsch GH, et al. Parametric T2 and T2* mapping techniques to visualize intervertebral disc degeneration in patients with low back pain: initial results on the clinical use of 3.0 Tesla MRI. *Skeletal Radiol.* 2011;40:543–51. <https://doi.org/10.1007/s00256-010-1036-8>.
36. Noebauer-Huhmann IM, et al. Sodium MR imaging of the lumbar intervertebral disk at 7 T: correlation with T2 mapping and modified Pfirrmann score at 3 T—preliminary results. *Radiology.* 2012;265:555–64. <https://doi.org/10.1148/radiol.12111920>.
37. Liang X, et al. Feasibility study for evaluating lumbar intervertebral disc degeneration using histogram analysis of T2* values. *Eur Spine J.* 2020;29:2600–8. <https://doi.org/10.1007/s00586-020-06476-7>.
38. Ishikawa T, et al. Evaluation of lumbar intervertebral disc degeneration using T1 rho and T2 magnetic resonance imaging in a rabbit disc injury model. *Asian Spine J.* 2018;12:317–24. <https://doi.org/10.4184/asj.2018.12.2.317>.
39. Takashima H, et al. Correlation between T2 relaxation time and intervertebral disk degeneration. *Skeletal Radiol.* 2012;41:163–7. <https://doi.org/10.1007/s00256-011-1144-0>.
40. Takashima H, et al. Lumbar disc degeneration assessment using T2* relaxation time with ultra-short TE. *Magn Reson Imaging.* 2020;73:11–4. <https://doi.org/10.1016/j.mri.2020.07.004>.
41. Kolf A-K, et al. T2* mapping of ovine intervertebral discs: normative data for cervical and lumbar spine. *J Orthop Res.* 2016;34:717–24. <https://doi.org/10.1002/jor.23071>.
42. Siemionow K, An H, Masuda K, Andersson G, Cs-Szabo G. The effects of age, sex, ethnicity, and spinal level on the rate of intervertebral disc degeneration. *Spine.* 2011;36:1333–9. <https://doi.org/10.1097/BRS.0b013e3181f2a177>.

Publisher's Note

Springer Nature remains neutral with regard to jurisdictional claims in published maps and institutional affiliations.

Ready to submit your research? Choose BMC and benefit from:

- fast, convenient online submission
- thorough peer review by experienced researchers in your field
- rapid publication on acceptance
- support for research data, including large and complex data types
- gold Open Access which fosters wider collaboration and increased citations
- maximum visibility for your research: over 100M website views per year

At BMC, research is always in progress.

Learn more biomedcentral.com/submissions

